2013 HASP Mission

SCARLET HAWK I

Abstract:

"SCARLET HAWK – I", the proposed HASP payload to be built by IIT's AIAA student chapter, is a test platform for development of future CubeSat-type missions. The payload subsystems are comprised of an onboard computer, power management, sensor packages including GPS and image capturing, and communications. The 2013 mission includes two scientific experiments investigating GPS tropospheric error and measuring stratospheric methane concentrations.

AIAA ILLINOIS INSTITUTE OF TECHNOLOGY

ACKNOWLEDGMENT

On behalf of AIAA-IIT's Space Technology Program, I would like to thank LSU and the 2013 HASP coordinators for providing our students with the opportunity to work on such an ambitious project. Greg Guzik, Doug Granger, and Michael Stewart deserve special recognition for their tremendous commitment in time and energy in order to ensure a successful mission. We would like to express our gratitude to Keith Bowman and IIT's MMAE Department for providing essential guidance and resources without which we could not have gotten this far. We also owe our accomplishments this year to the generous funding from the Armour College of Engineering Themes Committee, that allowed us to take the trip to Palestine, TX this summer.

Lastly, I would like to thank each and every team member who contributed their effort and talents to this project. There has not been a single day that I have not been impressed by their technical ability and their drive to do great works. It has been an honor to spend my time with them and I am proud to call them my colleagues.

Peter Kozak

AIAA-IIT Space Tech Program

TABLE OF CONTENTS

LIST OF FIGURES

CHAPTER 1
INTRODUCTION

1.1 Background

The student chapter of the American Institute of Aerospace and Aeronautics at IIT created its high altitude ballooning team early in 2012. The team began with very little experience building high altitude payload and few resources. In the year since then, the dedicated team members have spent on average about 10-20 hours a week, developing skills in areas often outside of their disciplines and making tremendous progress. IIT's first balloon payload, which was launched in spring of 2012, included a simple sensor package and a data logging computer. At that point, the next goal for the team was to work on a new project that would allow the members to build upon all that was learned from the previous flight. A HASP mission was decided upon as the next logical step.

Over the past year, an interdisciplinary team of undergraduates and graduate students developed SCARLET HAWK I, AIAA-IIT's first HASP payload. The payload comprised of several electrical subsystems, including power management, a sensor package, on-board cameras, and communications capability in flight. The team also designed a structure to contain the payload electronics and efficiently save space and weight. Throughout the design process and mission, AIAA-IIT members developed their technical abilities with respect to electronics design, computer aided modeling, and hands on manufacturing techniques. As an entirely student-run project, team members had the opportunity to try novel ideas, make mistakes, and learn from them.

1.2 Mission Goals of SCARLET HAWK I

SCARLET HAWK I was developed to be a continuation of past successes in developing remote sensing and communications payloads capable of surviving near-space conditions. The payload was also intended serve as a testbed for the development of more refined autonomous, multi-mission high altitude payloads. The proposed payload included two separate experimental setups and an image capturing package, which was designed to demonstrate the ability to take and transmit images and cope with severe bandwidth limitations. With this in mind, the following goals were formulated for AIAA-IIT's first HASP mission:

1. Measure the index of refraction with respect to altitude in order to validate GPS error models within the troposphere.

2. Measure concentrations of water vapor and greenhouse gases such as methane and carbon dioxide.

3. Capture images at float, store the images on-board, and send the images through the HASP serial connection, utilizing a Reed-Solomon error mitigation algorithm.

CHAPTER 2

EXPERIMENTAL RESULTS

2.1 Validation of Tropospheric Error Models for GPS

2.1.1 Introduction.

Measurements taken by GPS receivers are subject to multiple errors that result from signal delays and distortions due to the ionosphere, troposphere and multipath, receiver and satellite clock errors, inaccurate ephemeris data, and an inadequate number of visible satellites. Algorithms to estimate position fixes from GPS measurements are designed to mitigate the effect of these errors by correcting for them (in the case of clock and ephemeris errors) or by modeling them (in the case of Tropospheric and Ionospheric errors). The models, however, are generalized from assumptions and extrapolations for the index of refraction and do not provide the level of accuracy required for certain experiments. The tropospheric error model depends on variables that can change drastically depending on the day and time of measurement. The purpose of this experiment, therefore, is to validate the existing tropospheric error model by measuring the index of refraction as a function of altitude in real time and comparing resulting delays due to this refraction to the delays predicted by the existing models such as the Hopfield Model [5] [6] [7].

The majority of the signal delay occurs in the region of the earths atmosphere between 0 km MSL and 42 km MSL, which contains the troposphere. The content of the atmosphere at low altitudes causes a variation in the path of propagation of radio signals due to refraction of the signals. The effect of refraction on the propagation of radio signals is shown in Figure 2.1.

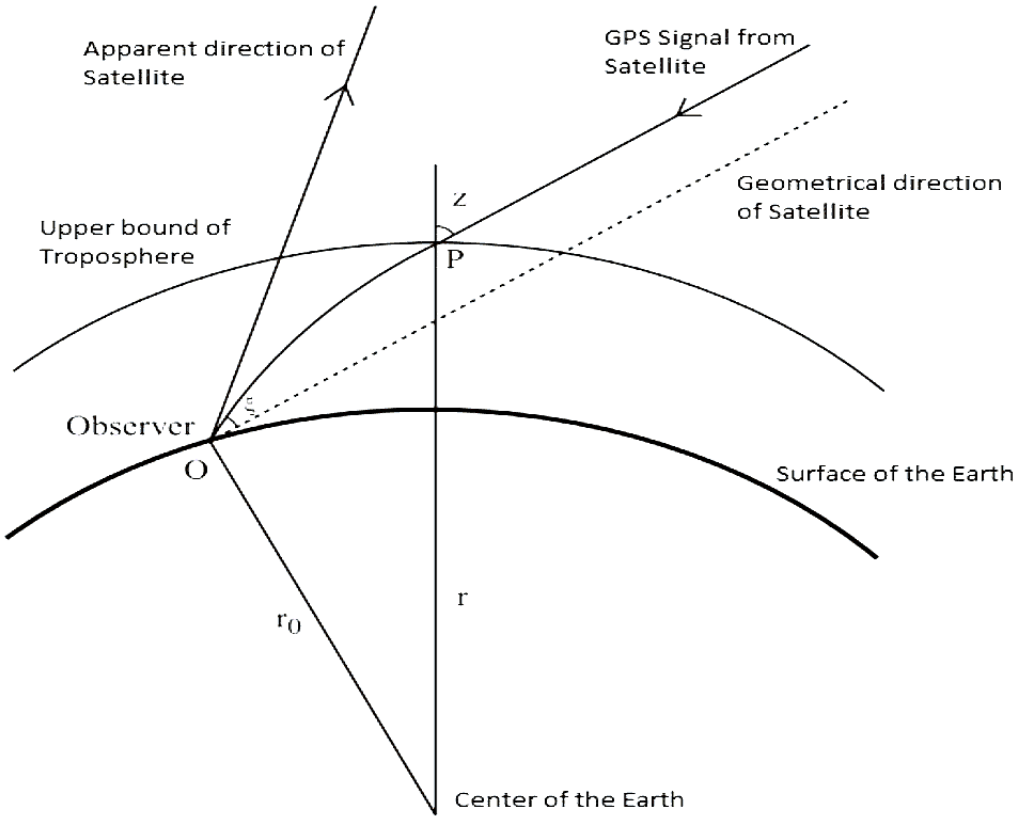

Figure 2.1. Diagram showing how electromagnetic signals are affected by refraction as they pass through the lower atmosphere. [4]

The Tropospheric Error affecting a GPS measurement consists of two primary parts, the Wet Tropospheric (TW) delay and the Dry Tropospheric (TD) delay. The wet tropospheric delay is the major contributing factor up to an altitude of 12 km MSL due to the existing water vapor whereas the dry tropospheric delay contributes the most at altitudes above 12 km MSL. The total Tropospheric Error (T) is calculated by adding up the two components. Tropospheric error for a radio signal traveling along the path of a 90 degree Elevation angle, an angle measured from the horizon, can be estimated by the following equation:

$$T = 10^{-6} \int [N_D(h) + N_W(h)]dh \tag{2.1}$$

where T is the total Tropospheric error (meters), N_D is the dry component of the index of refraction, N_W is the wet component of the index of refraction and h is the height from the receiver (in meters).

The challenge is to accurately calculate the dry and wet components of the indices of refraction in order to be able to achieve an accurate result for the tropospheric error. These components can be calculated using equations derived by Rueger [11]:

$$N = 77.6890\,\frac{P}{T} \;-\; 6.3938\,\frac{P_W}{T} \;+\; 3.7546 * 10^5\,\frac{P_W}{T^2} \tag{2.2}$$

where N is the total index of refraction, P is the total pressure (in millibars), PW is the partial pressure of water (millibars), T is the absolute temperature (K). The partial pressure of water vapor can be calculated by using the equations derived by Buck [1]:

$$e_{sat} = 6.1121\,(1.0007 + 3.46 * 10^{-6}\,P_o)\,e^{\frac{17.502\,T_o}{T_o + 240.97}} \tag{2.3}$$

$$P_{Wo} = e_{sat}\left[1 - (1 - RH)\,\frac{e_{sat}}{P_o}\right]^{-1} RH \tag{2.4}$$

where e_{sat} is the saturation vapor pressure (millibars), RH is the relative humidity, P_{Wo} is the partial pressure of water vapor (millibars).

2.1.2 Analysis Procedure.

The experimental setup consisted of three sensors measuring the atmospheric pressure, temperature and humidity against the altitude of the payload, also recorded through GPS measurements.

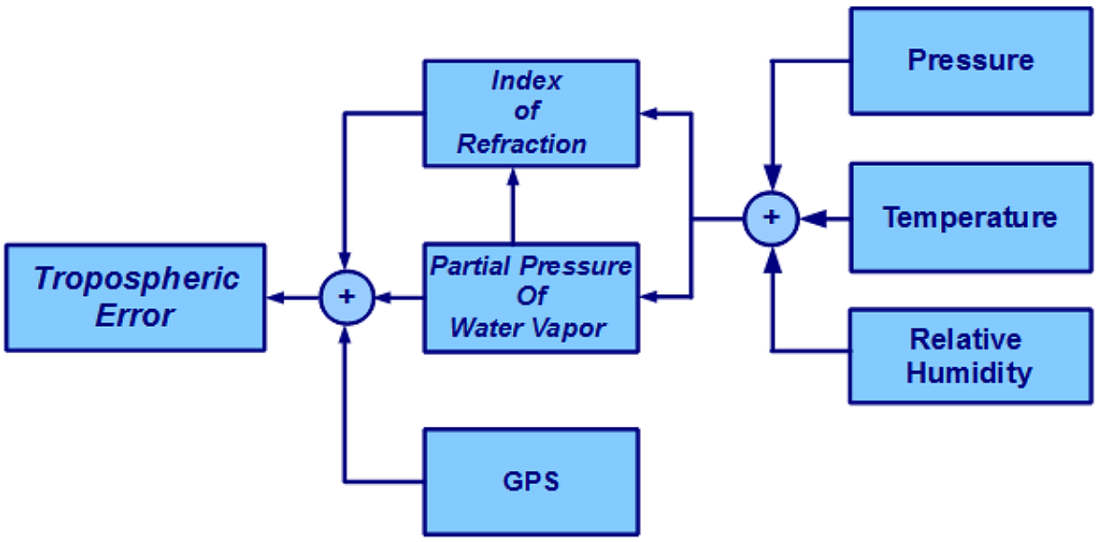

Figure 2.2. Representation of the experimental setup for tropospheric error measurement.

The analysis procedure is as follows:

1. Extract data necessary to calculate index of refraction and tropospheric error from the file

2. Filter out blank spaces in data (i.e. NaN values) and remove any anomalous data.

3. Once data is pre-processed, calculate the index of refraction

2.1.3 Results and Discussion.

The analysis conducted required a few critical decisions in order to extract valid results. Due to sparsity of data available and issues with time synchronization, there was a significant amount of anomalous data in the ascent and descent phases of the flight. Therefore data collected during the steady phase of flight was analyzed. The results still are inconsistent due to possible errors in the data used, regardless of significant pre-filtering.

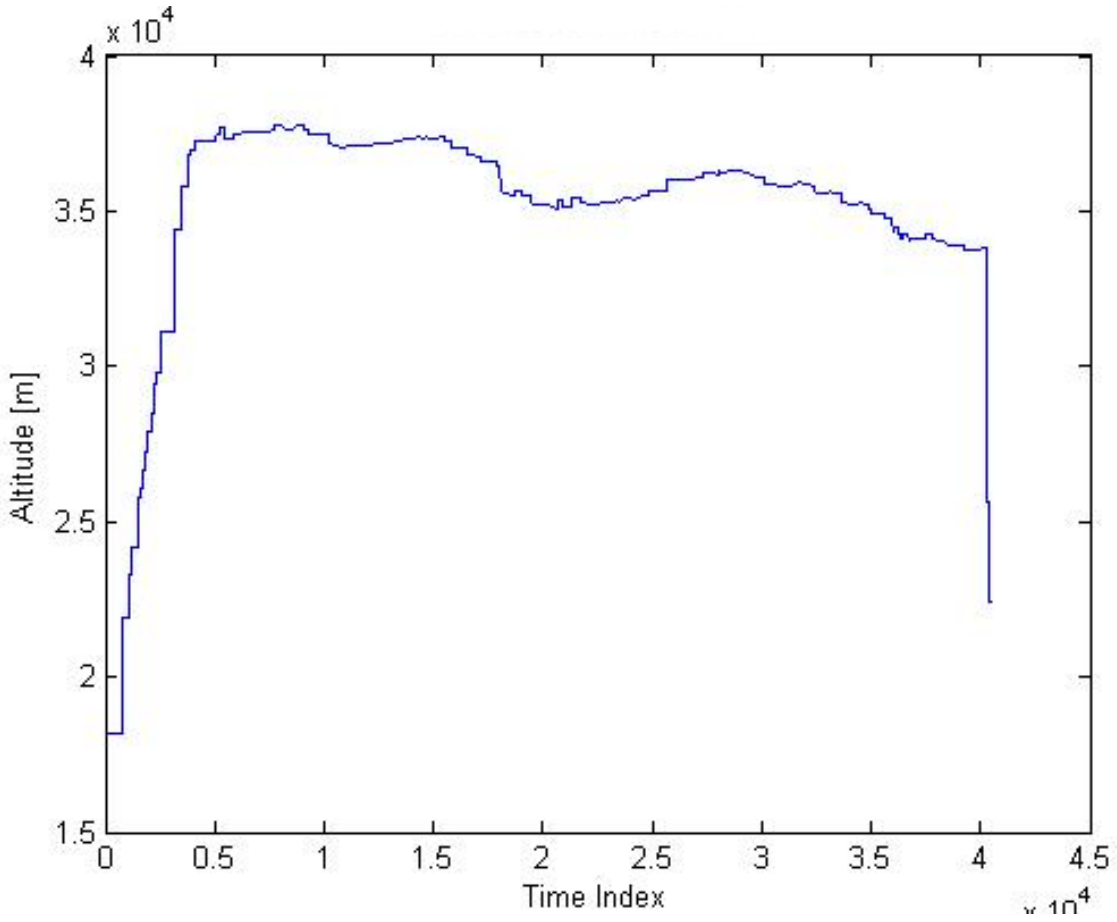

Figure 2.3. Altitude vs time index (in seconds

Pressure, temperature, relative humidity data was used to calculate the index of refraction (N). The pressure and temperature data followed trends as known in scientific literature with slight variations. However, the relative humidity (RH) data, which is one of the most critical elements in evaluating N, was inconsistent. This significantly affected the calculations for index of refraction. A noticeable relation between trends of change in altitude and change in index of refraction is visible. For the ascent and descent phases of flight, as the altitude increases the value of N decreases and vice-versa. This is because the moisture content of air decreases as altitude increases and therefore reduces the possibility of refraction incidences. During the steady phase of the flight at very high altitudes, the value of N held relatively constant. However, the values are constantly below N = 1. The index of refraction of vacuum is 1, meaning that a signal does not get refracted. Values below one should not be possible for the type of signal frequencies (L1 GPS frequency) and signal power in use. A best guess attempting to reason the occurrence of this error is anomalous relative humidity data.

A final step of analysis, integrating index of refraction over the signal path to calculate the actual tropospheric error, is not possible due to three reasons. The biggest reason for the inability to calculate tropospheric error is the significant lateral movement of the balloon during the flight phase. An accurate model of error was contingent upon multiple data points being collected at close locations, i.e. when the lateral motion of the balloon was slow. For this HASP flight, the balloon traveled long distances over the duration of the mission. Adding the lack of data to the balloons motion negated any chance of calculating a meaningful tropospheric error model. Another major reason is the lack of means to differentiate between different GPS satellites. And the final reason is the error in evaluating index of refraction.

The team was unsuccessful in evaluating and comparing tropospheric error to

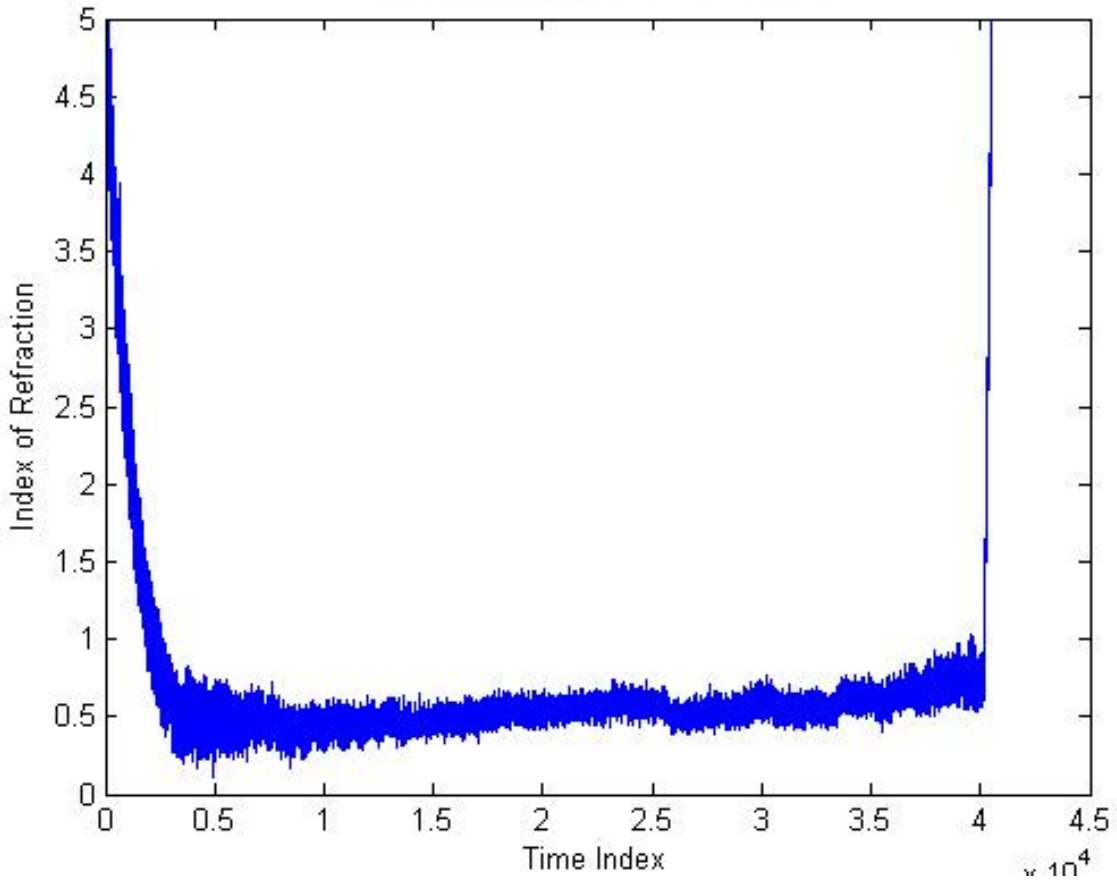

Figure 2.4. Index of refraction vs. time index (in seconds)

widely accepted error models. There were multiple events gone wrong that caused a stack effect in rendering the data invalid for calculating the tropospheric error. However, some results were successfully obtained from the data available for analysis. After significant pre-filtering, tentative values for the index of refraction as a function of altitude were obtained. These values followed general trends expected of the index of refraction within an approximate range of the true values of index of refraction and would have been much more accurate given a functioning humidity sensor. This result validated the choice of mathematical expressions used to evaluate the index of refraction. For these reasons, the experiment can be called a partial success.

2.2 Measurement of Stratospheric Methane and Water Vapor

2.2.1 Introduction.

Methane is the most common hydrocarbon trace in the atmosphere, which along with water vapor, contributes significantly to the Earths greenhouse effect. In the last 50 years, there has been a yearly 1% increase in stratospheric water vapor. [2] Likewise, up to a 15% increase in atmospheric has been measured from 1978 to 1998 with significant variations at different altitudes. [10] In order to better predict further increases and their effect on climate, a model has been developed to predict the concentrations of methane and water vapor at different altitudes.

$$C\,H_4 + 2\,O_2 \;<=>\; 2\,H_2\,O + C\,O_2 \tag{2.5}$$

The thermodynamic state of the surroundings must be known, including pressure, temperature, and gas concentrations. Since the relative concentration of oxygen remains nearly constant with altitude, the absolute concentration may be calculated from the pressure. In Eq. 1, the reversible stoichiometric reaction shows atmospheric methane reacts with oxygen to produce water vapor and carbon dioxide. The reaction rate is determined by the relative concentrations of the reactants and the temperature at which the reaction takes place. Eq. 2 and Eq. 3 are the governing equations where [A] is the concentration of some specie A, the Greek letters are the number of moles produced or consumed per reaction, and reaction constants k are found using the Arrhenius equation of equilibrium.

$$k_+[C\,H_4]^\alpha[O_2]^\beta \;= k_-[H_2\,O]^\sigma[C\,O_2]^\tau \tag{2.6}$$

$$k = A\, e^{-(\frac{E_a}{RT})^{\gamma}} \tag{2.7}$$

If the system is taken to be at steady state, which is a reasonable assumption, all time derivatives are defined to be zero and the methane concentration can be found simply using the equation:

$$[C\,H_4] \;=\; \left[\frac{k_{-}[H_2\,O]^{\sigma}[C\,O_2]^{\tau}}{k_{+}[O_2]^{\beta}}\right]^{\frac{1}{\alpha}} \tag{2.8}$$

2.2.2 Experimental Setup.

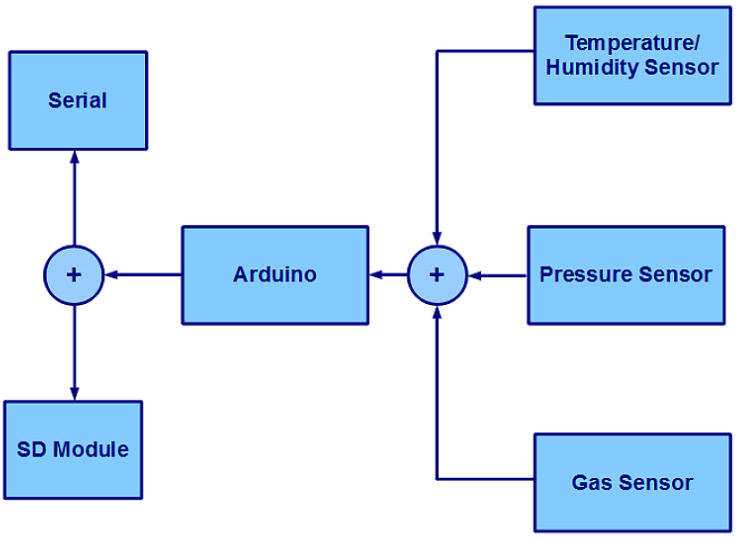

Figure 2.5. Representation of the experimental setup for methane gas measurement.

The sensor package contained on SCARLET HAWK I was designed to measure gas concentrations of methane, carbon dioxide, water vapor, as well as temperature, pressure, and humidity. This was accomplished using a sensor package fixed at the top of the electronics stack and open to the outside environment. Since the goal was to measure the methane concentration and thermodynamic properties with respect to altitude, the sensor package was designed to take data measurement during the ascent portion of the HASP mission as well as to take some data shortly before termination. This would allow the model to be validated for a full altitude profile.

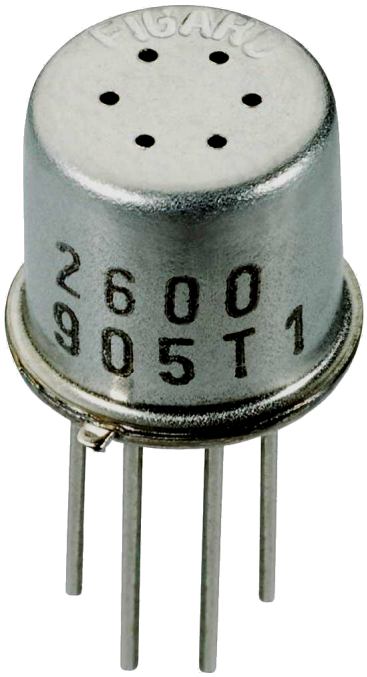

Figure 2.6. Figaro TGS 2600 gas sensor installed as part of SCARLET HAWK I's sensor package.

2.2.3 Results and Discussion.

While measuring the temperature, pressure, and relative humidity was a rather straightforward objective that had been done on previous high altitude missions, measuring gas concentrations was a different matter. A Figaro TGS 2600 gas sensor was chosen to measure gas concentrations due to its relatively good temperature characteristics. However, there were three major difficulties in measuring gas concentrations at high altitude: (1) many gas sensors such as ours utilize an infrared emitter inside in order to detect changes in transmission properties, which requires that the sensor maintain a defined temperature range; (2) most gas sensors are insensitive to the type of gas being detected; and (3) they are difficult to calibrate for a wide range of pressures. While these problems presented a serious challenge, the benefit of proceeding with the experiment was that the other sensors were already planned for the tropospheric error measurement experiment. Therefore, only the addition of a gas sensor was required, making the attempt worthwhile.

SCARLET HAWK I's sensor package successfully measured the temperature and pressure throughout the flight, with the exception of a brief period shortly before float. Accurate measurement of the relative humidity was difficult due to the limitations of our sensors. Particularly at low pressure, the temperature and humidity sensor was not able to detect water vapor with the required precision. As a result, the sensor output for the relative humidity was registered as less than zero, which is nonsensical. Surprisingly, the gas sensor performed well in the cold, low pressure environment and consistently provided data for the net concentration of carbon dioxide and methane throughout the flight. However, the lack of a humidity output as well as the inability to determine the concentrations of carbon dioxide and methane independently make a full analysis difficult. This information will prove useful for future attempts to validate methane concentration models using more reliable sensors.

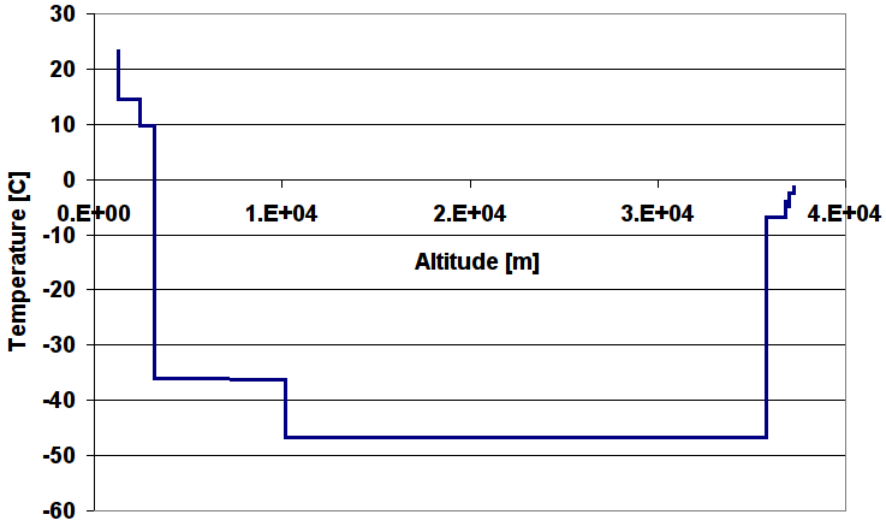

Figure 2.7. Plot of temperature vs altitude.

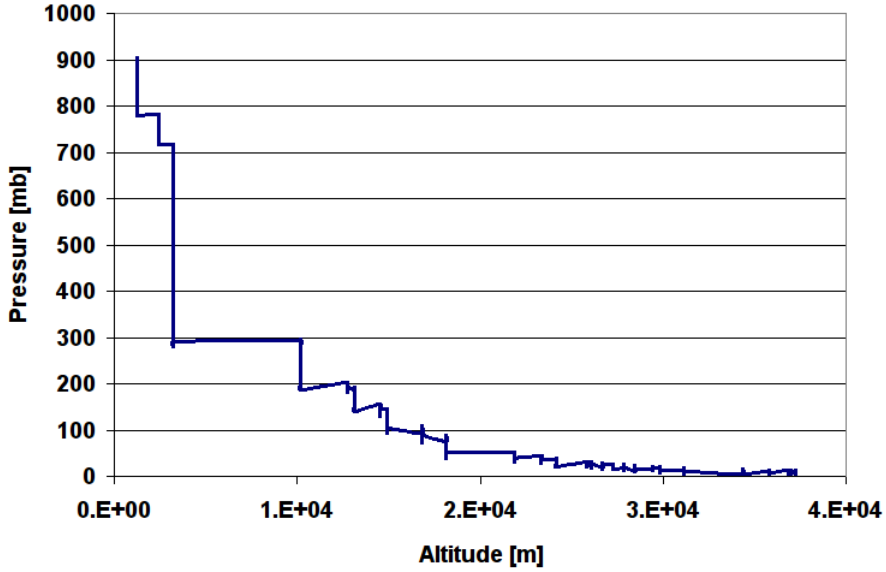

Figure 2.8. Plot of pressure vs altitude.

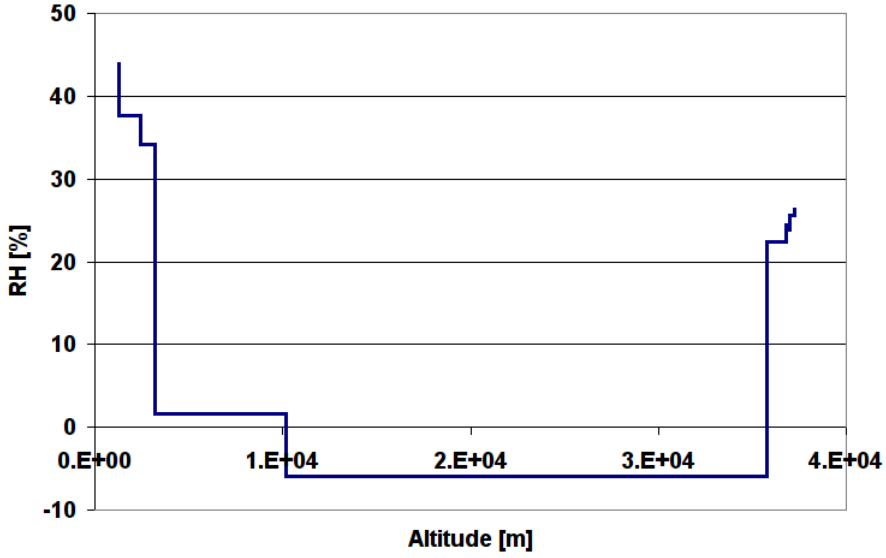

Figure 2.9. Plot of relative humidity vs altitude. The data in this plot is obviously incorrect since it passes below zero. This is likely due to pressure and temperature effects.

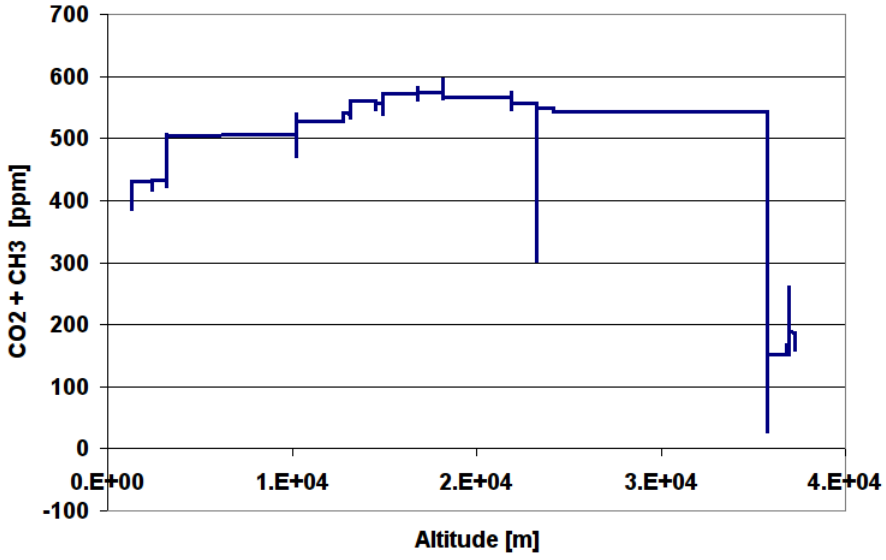

Figure 2.10. Plot of carbon dioxide + methane concentration with respect to altitude.

2.3 Image Capture and Transmission

2.3.1 Camera System Development.

Many high altitude balloon missions have included some form of photography or remote image capturing. This has typically required taking pictures that are saved to an internal memory inside the payload, and retrieved after the payload descends back to the ground. Apart from the risk of losing the payload with the data, it is also not possible to see the images until the payload is on the ground. However if the images can be converted into a data string and sent to a control station on the ground, then the information can be preserved and obtained earlier in the mission. Furthermore, for other types high altitude missions, including sounding rocket launches and CubeSat missions, real-time image transmission is a mission-critical requirement.

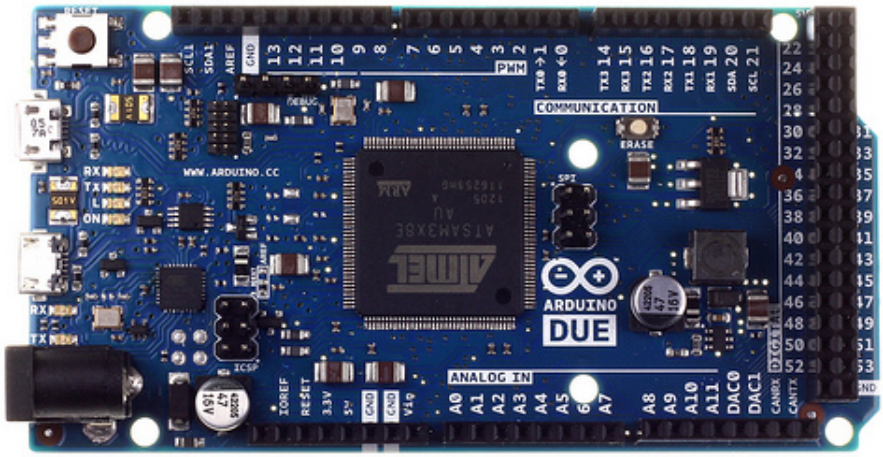

Figure 2.11. Arduino Due micro-controller used for the ICS.

The purpose of the ICS (Image Capture System) is to optimize the process of image capturing and transmission from a high-altitude payload such as a HAB

payload or even a CubeSat to a ground station. This will allow the ICS to stay within the narrow operating envelope defined by Baud rates, power consumption, and downtime limitations. This is achieved by powering down all other non-critical components, then using three cameras to capture images individually and transmit the image data using the HASP serial port. For these reasons, it was decided that an ICS be included in SCARLET HAWK I.

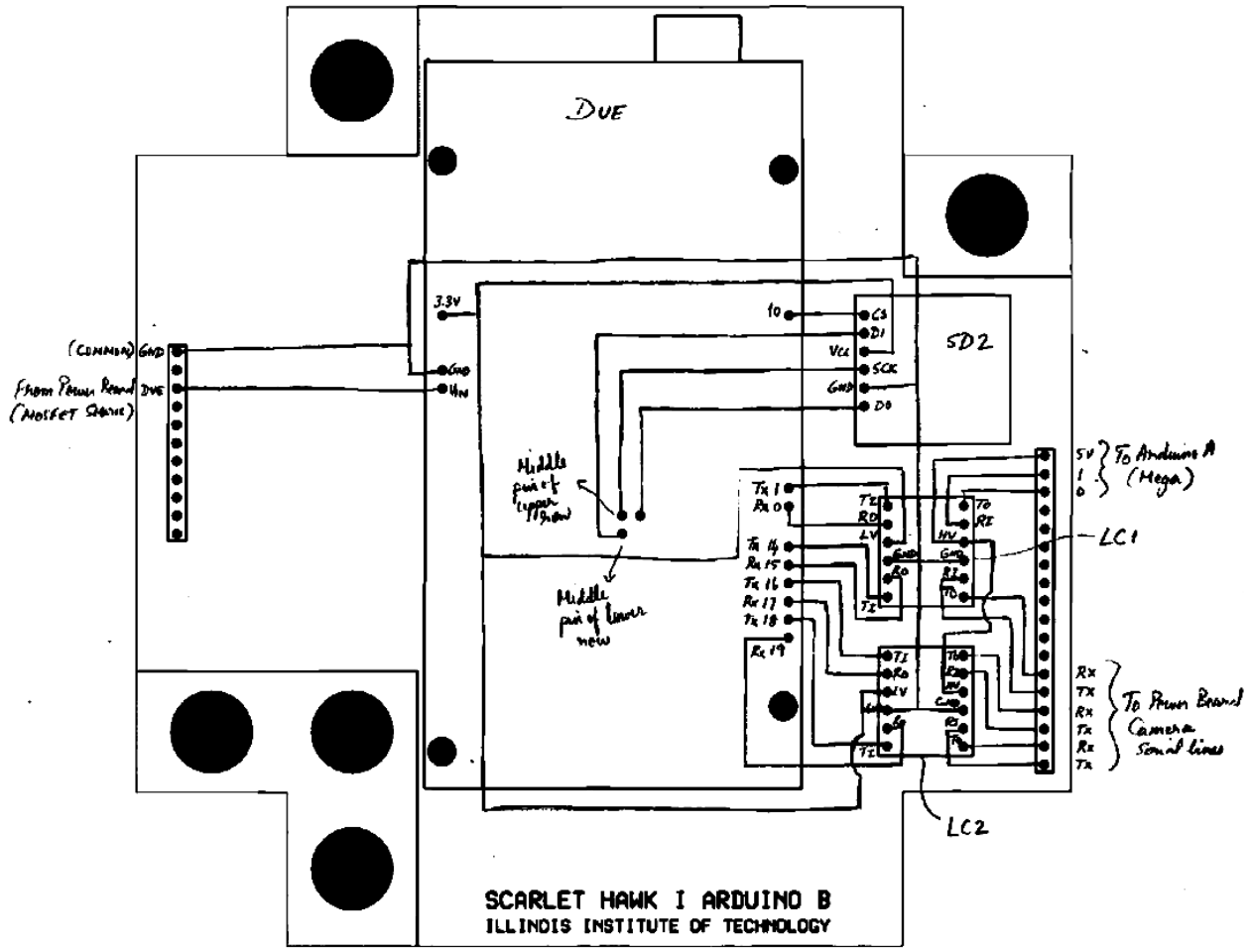

Figure 2.12. Representation of the experimental setup.

Several characteristics of the subsystem changed since the submission of the proposal in December, 2012. The most important of these changes was the use of a different micro-controller with a bigger SRAM and a more powerful microprocessor. The SRAM in the originally considered microprocessor (ATmega1280) was 8KB compared to 96KB in the microprocessor used for the flight (AT91SAM3X8E). The reason behind using the new microprocessor on board was that an encoding algorithm, a Reed-Solomon code, was necessary to include in the original design in order to ensure that the majority of image data would be recovered uncorrupted.

The Reed-Solomon algorithm implemented required at least 20KB of static memory to be able to do the encoding of the 6KB pictures that were to be sent as thumbnails to ground station. This change in microprocessor also required another important change in the design of the payload electronics. The Arduino Mega that was used as the master computer for the mission required serial communication at 5V, while the Arduino Due required 3V. Two level converters, to step down from 5V to 3V, had to be adapted for the serial communication between the cameras and Arduino B, and between Arduino A and Arduino B. The final EPS for the main board of the Image Capturing System is shown in Figure 2.12.

2.3.2 Results and Discussion.

At the beginning of this experiment, three objectives were set for this subsystem:

Table 2.1. ICS Objectives

Mission	Result
Capture of images in flight	Successful
Image processing and storage on-board	Successful
Image transmission in flight	Unsuccessful

In total, 506 pictures were taken throughout the flight. The system was configured so that the cameras take big pictures (40KB) during the entire flight and small pictures (6KB) whenever a command were received by the microprocessor. Both small and big pictures were found within the 506 pictures and they certainly follow a logical sequence.

(a) Hi-Resolution $\sim$ 40 KB Image

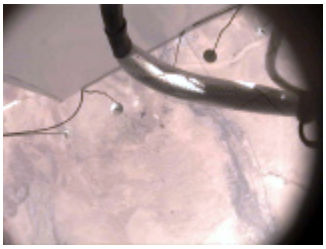

(b) Low-Resolution $\sim$ 6 KB

Figure 2.13. Examples of a high (a) and low (b) resolution image captured in flight.

Of the three cameras on board, two were fully functioning. However, one of the side cameras failed. The amperage stayed within the expected range, 0.19-0.2 amps, during the flight. This fact led us to think all the cameras were working properly. A post-flight analysis of the electronics in the payload, however, determined that the TX connection of one camera unsoldered during the flight. Therefore, none of the pictures taken by this camera were saved to the SD card on board.

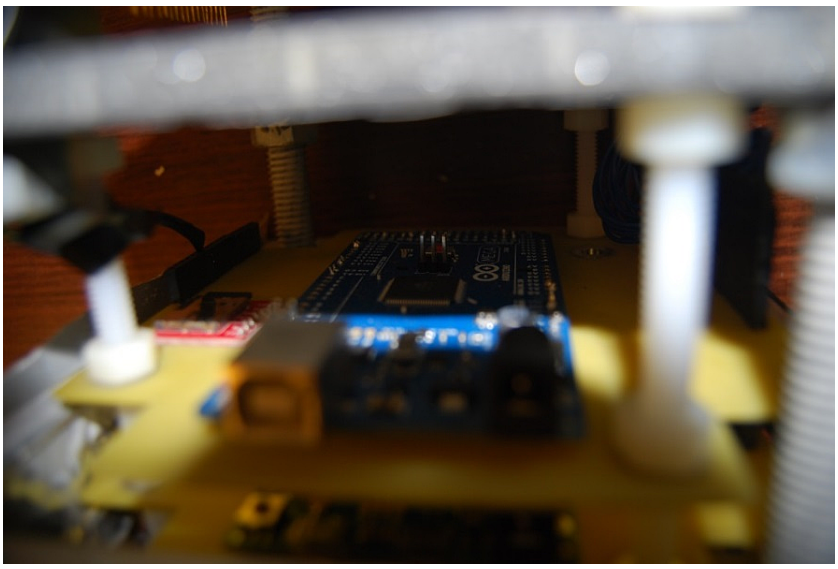

Figure 2.14. Picture of the Arduino A when the payload was opened for the first time following recovery.

As data transmission failed between the micro-controller in charge of transmitting the data to ground (Arduino A) and the micro-controller in charge of the image processing (Arduino B), our team was only able to see the pictures once the payload was recovered. All the pictures taken throughout the flight were successfully compressed and saved under the JPEG-2000 format. According to the recording rate, there was enough storage capacity for 102 hours of flight.

The code in the Arduino B worked properly during the flight test and the

actual flight. All of the 5 commands sent from ground station to switch from big to small pictures and vice versa were totally executed and processed by the micro-controller. The evidence for this can be observed in each of the three folders (one per each camera) containing exactly 5 small pictures that were to be used as thumbnails. Problems with the code run by the Arduinos as well as with the Reed-Solomon algorithm on board were discarded after confirming that the data in the SD card fully matched the logic behind these codes. Name sequence (files were name after a logical increasing sequence), timestamps and number of files showed that Arduino B successfully received the commands, managed to take, stored, encode and forward the pictures to Arduino A, but Arduino A did not receive the transmitted thumbnails.

The fact that every time that a command was sent to switch to small pictures the command was executed and the thumbnails encoded but the images were not going through HASP Channel suggested that a possible cause of the failure was in the communication between Arduino A and Arduino B. The only electrical component between both micro-controllers was the level converter. Once the region of the issue was identified, continuity was checked between all the TX and RX connections. Communication between the Transmission port of the Arduino B and the Reception port of the level converter proved to be working fine in a post-flight test. The connections between Arduino A and the level converter were also working properly after the flight. The entire system was run again and no communications issues were detected. It should be noted that the connection between both micro-controllers worked perfectly during the thermal-vacuum test. The failure in the level converter might have, then, been due to specific flight conditions.

The temperature range during the time the commands were sent was from 29C to 45C inside the payload while it stayed steady around 29C for the exterior temperature during the same period. During this time, the pressure also stayed close

to 10 millibars. Also, the payload design was found to be inefficient for rejecting heat, which resulted in a difference between interior and exterior temperature greater than 10C. All of these points then lead to the conclusion that the failure in this subsystem was due to the effect of environmental conditions (at the recorded altitude range between 37,130km and 37,700km) in the level converter between both Arduinos.

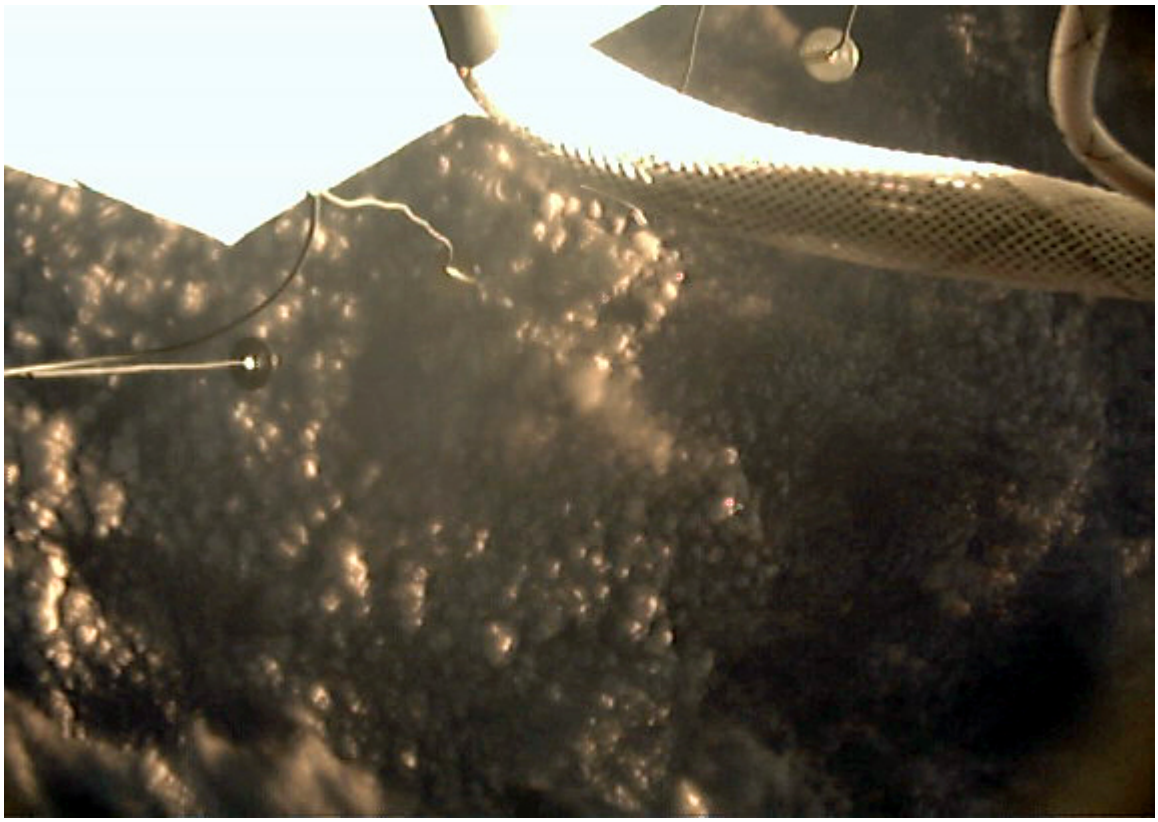

Figure 2.15. Downward view of the cloud cover below at float altitude.

(a) High resolution image of the horizon taken during float at 130,000 ft.

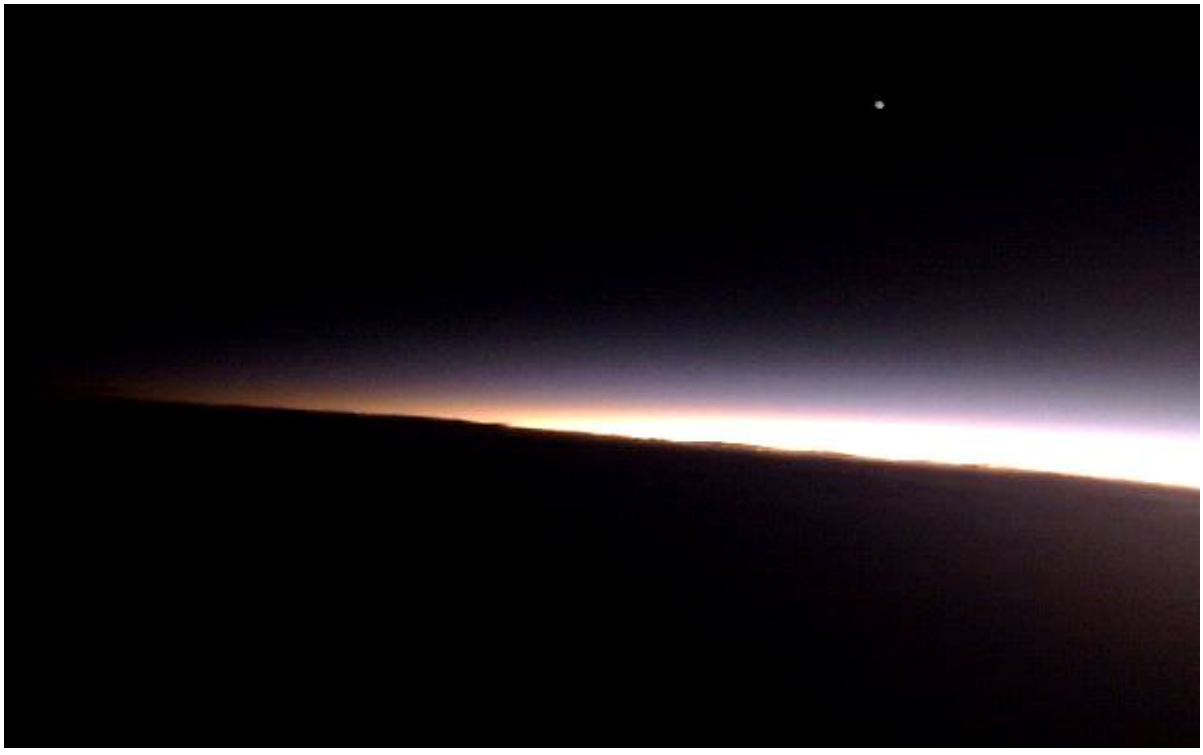

(b) Southwestern view at dusk, with Venus visible near the upper right corner.

Figure 2.16. Side view images taken during the flight.

(a) View of the sunset at 130,000 ft.

(b) View of the horizon and the ground below at sunset.

Figure 2.17. Side view images taken during the flight.

CHAPTER 3
PAYLOAD DESIGN EVALUATION

3.1 SCARLET HAWK I

The payload electronics was comprised of four printed circuit boards, containing the on board computer, power management system, image capture system, and sensing circuits. At different times throughout the mission, the payload ran on one of two different modes of operation: Sensor Mode or Camera Mode. This layout and mode of operation helped to conserve space, weight, and electrical power. Furthermore, utilizing a stacked system of printed circuit boards helped to minimize the number of free wires in the payload and likely prevented shorted circuits as well as other mishaps. The only major problem with this layout is that the stack had to be pulled out of the structure in order to reach the SD cards or any of the computer ports. The lack of practical accessibility to the hardware also made it more difficult to replace malfunctioning electronics during the testing and integration phase.

Two Arduino microcomputers provided all on-board computing, with an Arduino Mega serving as the master computer that controlled whether the payload was in sensor or camera mode. An Arduino Due was required to control the image capture system since more SRAM was needed for the Reed-Solomon algorithm. While this was actually a good idea in itself, problems emerged due to the fact that the Arduinos operated using different serial voltages. This required the inclusion of a level converter that later failed, causing problems for the GPS and image capture systems later on.

In retrospect, we realize that carbon fiber was not a good material to use for the entire structure. It carried a considerable portion of the overall cost of the payload and made thermal management difficult. Painting the surface of the carbon

fiber was found to be nearly impossible, with the paint actually peeling off during thermal-vacuum testing. Eventually, tape was used to cover the dark colored exterior in order to minimize sunlight absorption. Carbon fiber also proved to be relatively difficult to work with, since manufacturing errors were very expensive because of the cost of the material. In terms of strength, SCARLET HAWK I's structure was clearly over-engineered for the actual mission requirements.

One of our most serious errors was assuming that the cold temperatures were most likely to cause problems with electronics. During testing as well as the mission, overheating was likely the culprit behind some of the malfunctions that occurred during the flight. One of the main failures, for example, was the level converters in the image capture system and this was due to overheating. One way of tackling this issue would be attaching heat sinks to the critical components of the system and developing a way of rejecting heat out of the payload.

3.2 Proposed Changes for SCARLET HAWK II

1. A more practical access to the memory cards and uploading ports should be implemented in future payloads, likely using easily removable panels .

2. More effort should focus on heat management in general and rejection of heat from critical components in particular.

3. Effort should be made to quickly produce prototype electronics, so they can undergo rigorous testing early in the design process. Testing their performance at different critical conditions (e.g. high temperatures) would certainly avoid problems like the one of the GPS and the level converters.

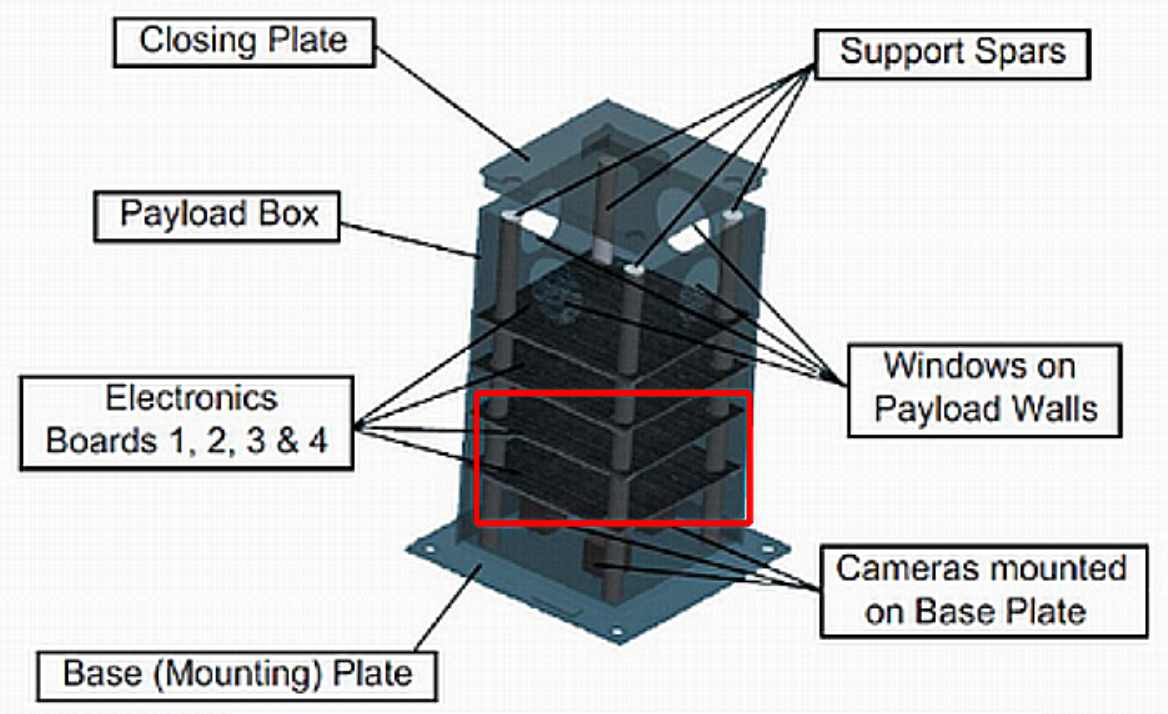

Figure 3.1. Region where the ports and SD cards were located inside the red box, out of reach of the top or bottom openings.

4. In order to eliminate the need for level converters (that can fail), all on-board computers should operate with a common serial voltage.

5. The management structure of future teams should include greater delegation of responsibilities. Emphasis should be placed on developing leadership skills throughout the team from top to bottom. These skills are important for engineers and are not learned in the classroom.

6. Design schedules should be planned more aggressive deadlines, since the team lost a great deal of manpower once the summer break had begun.

7. Future structural design should favor simpler construction and more commonly available materials. Mechanical fasteners should be chosen over less reliable and more permanent epoxying.

8. More focus and less broad mission objectives should be aimed at for future endeavors. This will leave more energy and resources to successfully accomplish all of the mission goals.

3.3 Looking Forward

SCARLET HAWK I served as AIAA-IIT's first payload for a HASP mission and collected data for several missions simultaneously. In the areas where the payload functioned well and successfully completed its goals, SCARLET HAWK I proved the teams ideas and designs. The aspects of the payload that did not perform satisfactorily also allowed the team to understand our mistakes and develop alternative designs for future missions. Above all, AIAA-IIT was able to pass integration and fly on the 2013 HASP mission without a critical system failure. We are now familiar with the process of designing a payload for a HASP mission and understand the opportunities that will be available next year.

Now that the mission has been completed, the hard work of planning for a HASP 2014 mission must begin. This work has been detailed in a proposal which will be delivered to HASP coordinators on December 20, 2013. With the beginning of a new year, AIAA-IIT's Space Technology Program will continue to actively recruit and train new members. These new members can be expected to play a large part in the design of SCARLET HAWK II and will apply the lessons we have learned this year.

APPENDIX A

2013 AIAA-IIT TEAM DEMOGRAPHICS

Table A.1. AIAA-IIT Demographics Data

Last Name	First Name	Gender	Ethnicity	Race	Status	Disability
Arnaout	Abdulrhaman	M	Non-Hispanic	Caucasian	Grad	N
Borate	Shalmikraj	M	Non-Hispanic	Indian	Grad	N
Finol	David	M	Hispanic	Latino	Undergrad	N
Garcia	Jesus	M	Hispanic	Latino	Undergrad	N
German	Joshua	M	Non-Hispanic	African	Undergrad	N
Grimaud	Lou	M	Non-Hispanic	Caucasian	Grad	N
Haider	Qasim	M	Non-Hispanic	Asian	Undergrad	N
Javier	Miguel	M	Non-Hispanic	Asian	Undergrad	N
Katre	Aniruddha	M	Non-Hispanic	Indian	Grad	N
Kozak	Peter	M	Non-Hispanic	Caucasian	Grad	N
Lin	Senbao	M	Non-Hispanic	Asian	Grad	N
Manotas	Rodolfo	M	Hispanic	Latino	Undergrad	N
Page	Corey	M	Non-Hispanic	Caucasian	Undergrad	N
Rutenbar	Colin	M	Non-Hispanic	Caucasian	Undergrad	N
Singh	Manpreet	M	Non-Hispanic	Indian	Grad	N
Venet	Teva	M	Non-Hispanic	Caucasian	Undergrad	N
Vitto	Raisa	F	Non-Hispanic	Indian	Grad	N

APPENDIX B

HASP 2013 STUDENT IMPACT

B.1 Impact Statements

B.1.1 Abdulrhaman Arnaout - EECE Graduate Student.

HASP project made me realize how vast studying the behavior of electronic pieces on high elevations is. So I could now imagine how different it will be in the far space! My experience with Scarlet Hawk team was amazing; I have seen so many students working very hard on this project despite the fact that they have so much load coming from their other classes, and this project doesn't count toward their degree; and yet, they were always excited, enthusiastic, and happy! The moment when you try what you built, and it does work, you just feel fantastic.

B.1.2 David Finol - MMAE Undergraduate Student.

The HASP program has certainly helped me develop my professional skills and get a taste of what it will be like after school. The fact that there is no second chance in a flight and that there are efforts of an entire team in risk truly pushes me to make the most out of the flight. The program allows us to get acquainted with space-like conditions and definitely gives the hands-on experienced to tackle all the challenges brought by those conditions. The very professional and punctilious way Dr. Guzik and his team manages the program also made it a fruitful experience for me.

B.1.3 Qasim Haider - EECE Undergraduate Student.

Working in HASP 2013 has had such an immense affect on my academic life, I have learned so much while working on the project. It has really broadened the horizons of my mind and taught me that 'sky is the limit!'

B.1.4 Miguel Javier - MMAE Undergraduate Student.

The HASP program that I have been a part of has allowed me to put to use my CAD knowledge and design class to be able to design and build the payload for the project. Additionally being able to go through the design build process all the way through the completion of the project has allowed me to see the project through until the end.

B.1.5 Aniruddha Katre - MMAE Graduate Student.

HASP was a very exciting experience because it gave me the chance to help take a product through the complete design, manufacturing, assembly and testing phase. Also, the the experience of working in a team environment with the freedom to innovate and apply the knowledge gained from academics in a practical setting relevant to my academic background was invaluable.

B.1.6 Senbao Lin - MMAE Graduate Student.

Working on AIAA-IIT's HASP mission has:

1. Enhanced my communication skills
2. Improved my time management skills
3. Gave me new perspective to look at technology

B.1.7 Rodolfo Manotas - MMAE Undergraduate Student.

Participating in HASP allowed me to get a better understanding of how engineering knowledge can be applied to a project involving designing an experiment. Working in a team with graduate students and other students both below and above

my level, with multiple talents and in different disciplines, gave me a great deal of experience and gives me an idea of what my future challenges in engineering could be like. Finally, being able to interact with teams from other universities helped us to see things from other points of view and also to exchange a few ideas among each other.

B.1.8 Colin Rutenbar - CAEE Undergraduate Student.

HASP definitely gave me a an outlet for skills outside of my major and to help a team accomplish a goal. It has prepared me for working in an IPRO as well as working with multiple levels of education (from freshmen to PhD candidates) and to work in a multicultural group.

BIBLIOGRAPHY

[1] Buck, A. L. (1981). New equations for computing vapor pressure and enhancement factor. *Journal of Applied Meteorology, 20(12)*, 1527-1532.

[2] Kley, D., & Phillips, C. (Eds.). (2000). *SPARC assessment of upper tropospheric and stratospheric water vapour*. SPARC office.

[3] Kuo, K. K. (1986). Modeling Oxidation Chain Reaction. *Principles of combustion.*

[4] Hohenkerk, C. Y., & Sinclair, A. T. (1985). *The Computation of an Angular Atmospheric Refraction at Large Zenith Angles.* HM Stationery Office.

[5] Hopfield, H. S. (1969). Two-quartic tropospheric refractivity profile for correcting satellite data. *Journal of Geophysical research, 74(18)*, 4487-4499.

[6] Hopfield, H. S. (1971). Tropospheric effect on electromagnetically measured range: Prediction from surface weather data. *Radio Science, 6(3)*, 357-367.

[7] Hopfield, H. S. (1972). *Tropospheric refraction effects on satellite range measurements.*

[8] Mangum, J. (2009). Atmospheric refractive signal bending and propagation delay. *Report, National Radio Astronomy Observatory (NRAO).*

[9] Milbert, D. (2012). Sources of Errors in GPS. *GPS Explained: Error Sources.*

[10] Riese, M., Grooss, J. U., Feck, T., & Rohs, S. (2006). Long-term changes of hydrogen-containing species in the stratosphere. *Journal of atmospheric and solar-terrestrial physics*, 68(17), 1973-1979.

[11] Rueger, J. M. (2002). Refractive index formulae for electronic distance measurement with radio and millimetre waves. *Unisurv Report S-68, School of Surveying and Spatial Information Systems, University of New South Wales, UNSW SYDNEY NSW, 2052*, 1-52.

[12] Stewart, M. F. (2009). Time and Position Data String Serial Latency Measurements. *HASP Technical Report 2009-01*